JOURNAL OF GEOPHYSICAL RESEARCH, VOL. 96, NO. A2, PAGES 1351–1367, FEBRUARY 1, 1991

Limits to the Lunar Atmosphere

T. H. MORGAN

National Aeronautics and Space Administration, Washington, D. C.

D. E. SHEMANSKY

Lunar and Planetary Laboratory, University of Arizona, Tucson

The presence of sodium and potassium on the Moon implies that other more abundant species should be present. Volatile molecules like H_2O are significantly more abundant than sodium in any of the proposed external atmospheric sources. Source mechanisms which derive atoms from the surface should favor abundant elements in the regolith. It is therefore puzzling that the Apollo ultraviolet spectrometer experiment set limits on the density of oxygen of $N_O < 5 \times 10^2$ cm^{-3}, and that the Apollo Lunar Atmospheric Composition Experiment data imply $N_O < 50$ cm^{-3} above the subsolar point. These limits are surprisingly small relative to the measured value for sodium. A simple consideration of sources and sinks predicts significantly greater densities of oxygen. It is possible but doubtful that the Apollo measurements occurred during an epoch in which source rates were small. A preferential loss process for oxygen on the darkside of the Moon is considered in which ionization by electron capture in surface collisions leads to escape through acceleration in the local electric field. Cold trapping in permanently shadowed regions as a net sink is considered and discounted, but the episodic nature of cometary insertion may allow formation of ice layers which act as a stabilized source of OH. On the basis of an assumed meteoroid impact source we predict a possible emission brightness of $\sim$ 50 R in the OH(A – X)(0,0) band above the lunar bright limb. A very uncertain small comet source of H_2O could raise this value by more than two orders of magnitude.

INTRODUCTION

Measurements of the abundance and scale of sodium and potassium in the lunar atmosphere were obtained for the first time in January 1988 [*Potter and Morgan*, 1988*a*]. *Tyler et al.* [1988] subsequently obtained measurements of Na in June 1988, and in October 1988 *Potter and Morgan* [1988*b*] found evidence of a distribution well beyond the scale of accommodated gas. These results are currently our point of reference for the presence of other possible species in the lunar atmosphere. Na and K may originate from both the regolith and meteoroids by impact vaporization [*Morgan et al.*, 1989], and from the regolith by solar–wind driven sputtering, photon stimulated desorption, and a very small contribution from diffusion[*Sprague*, 1990]. Neither element is a major constituent of the regolith (Table 1) or of the meteoroid population, and it is reasonable to ask if other more abundant volatile species are present in the lunar atmosphere as well.

The solar–wind sputters any species present in the regolith, and the yield is approximately proportional to the relative abundance of the element in the regolith, although the upper subsurface layers do evolve through subsequent chemistry. Solar photons also desorb regolith species at or near the top surface atomic layer. The population of infalling micrometeoroids is a source of volatiles. Recent upward revisions in the global influx of extraterrestrial material onto the upper atmosphere of the Earth [*Kyte and Wasson*, 1986], and more modest revision in the presumed abundance of volatiles in the meteoroid complex drawn from the analysis of the interplanetary dust particles (IDPs) result in an upward revision to the volatile supply rate to the surface of the Moon. Comets provide a significant source of H_2O but the observed component is long term episodic and the retained fraction is uncertain. A particular class of small comet hypothesized by *Frank et al.* [1986] forms a more steady source of enormous proportions, but is not included in our calculation of predicted measureable quantities, with the intent of calculating a conservative lower limit to H_2O input to the atmosphere.

One might expect that the constituents of the sunlit lunar atmosphere were identified during the Apollo program, but only night–time measurements of neutral species were possible on the surface of the Moon. A vacuum UV spectrograph on board the Apollo orbiter was able to search for an atmosphere away from the contaminated Apollo lander sites [*Fastie et al.*, 1973], but no species were detected. We are therefore in the peculiar position of having detected minor constituents in the atmosphere but none of the naturally more abundant species. The upper limit on the abundance of oxygen determined by the *Fastie et al.* [1973] experiment is particularly significant because this quantity is small relative to expectation from the measured abundance of Na. A neutral mass spectrometer experiment on Apollo 17, was limited to darkside measurements but no oxygen was identified. Since any plausible source process predicts much larger relative rates for oxygen, the requirement for a strong differential in loss rates presents a serious physical problem. Consideration of the obvious loss processes produces a predicted abundance of oxygen conservatively 1000 times larger than the upper limit set by the Apollo UV spectrometer measurements. We explore possible explanations for this unexpected development. In the following text we discuss the constraints implied by the observations on the possible sources and competing loss processes, with particular attention to oxygen.

Paper number 90JA02127.
0148-0227/91/90JA-02127$05.00

TABLE 1. Solar Wind Proton Sputtering Rate For Common Regolith Materials

Species	Regolith Abundance relative number	Source Rate 10^{+5} cm^{-2} s^{-1}
O	0.60	4.4
Si	0.17	1.2
Al	0.11	0.74
Ca	0.062	0.44
Fe	0.020	0.15
Mg	0.037	0.24
Na	0.0033	0.024
K	0.00035	0.0025

The Observational Evidence: Apollo Epoch Measurements

The Apollo program included instruments on both the surface of the Moon and in lunar orbit designed to detect possible atmospheric constituents. We shall consider the surface measurements first, followed by the measurements of the atmosphere obtained from the command and service module orbiting above the Moon, typically 100 km or less above the surface.

Surface Measurements

The Apollo lunar science experiment packages (ALSEP) attempted to measure the total pressure of the sunlit lunar atmosphere and to determine composition. The total pressure measurement was to be made with an ionization gauge (the Cold Cathode Gauge Experiment, hereafter, CCGE) which was included in the ALSEPs for three missions. The CCGE was a vacuum ionization gauge of conventional design in which the neutral species were ionized and the ion current measured. In the event, the in situ environment at the landing sites was so contaminated by invasive extralunar gases, both prompt and delayed, that only nighttime measurements were reliable. The CCGE experiment, in particular, was driven offscale by the approach of an astronaut. The derived daytime densities were 5–10 $\times 10^7$ atoms cm^{-3} [*Johnson et al.*, 1972], but the fraction of this that was native to the sunlit atmosphere of the Moon is unknown as is the degree to which the initial large flux of pollutant species and internal outgassing may have compromised the subsequent performance of the gauge.

The composition of the lunar atmosphere was to be determined with a neutral mass spectrometer (Lunar Atmospheric Composition Experiment, LACE) which was, unfortunately, placed at only one of the Apollo landing sites (Apollo 17). The neutral species were ionized near the entrance aperture and resulting ions separated with a mass spectrometer [*Hoffman et al.*, 1973]. The neutral gas spectrometer was also swamped by contaminant species during the lunar day, but nighttime and twilight measurements identified Ar, He, and possibly Ne. Weak signals at sunrise in the 15 and 16 amu channels were attributed to methane [*Hodges and Hoffman*, 1975]. The fact that a 16 amu component was not reported by the LACE experiment in the dark atmosphere has interesting implications for the physics of atomic oxygen in the atmosphere, as discussed below.

Measurements From the Command Service Module

Apollo missions 15 and 16 included a mass spectrometer, the lunar orbital mass spectrometer (LOMS), in the command and service module (CSM). H_2O and OH were detected but these species were attributed to the vapor cloud surrounding the spacecraft [*Hodges et al.*, 1972]. The prompt report on LOMS performance claimed that Ne was present, but subsequent analysis did not support this identification (R. R. Hodges, private communication, 1990). Mission 17 included an ultraviolet spectrometer (UVS) onboard the CSM. The spectrometer was used in an attempt to observe resonance scattering and fluorescence of solar radiation in the resonance transitions of H, H_2, O, C, N, CO, Kr, and Xe. The flux received by the spectrometer depends on the effective column of atmosphere in the line of sight to the spectrometer. For all species but H, the most sensitive measurements required a tangential viewing geometry looking above the subsolar point. For H the most sensitive measurement was performed during orbital insertion with a 550 km path length looking onto the Moon across the terminator with the surface in the field of view being dark. The orbit of the CSM was 45 to 73 km above the surface. *Fastie et al.* [1973] reported no emission in any of the above species away from the Apollo landing site. The only positive emissions observed were 2 hours after the landing of the lunar module. These were a faint emission in the 1304 Å O line and in one band of the CO fourth positive system(recent reanalysis has failed to confirm these results, according to P. D. Feldman, private communication, 1990]. During transearth coast, the UVS made measurements of stars, the geocorona, and other features including an H_2 cloud about the spacecraft from an H_2 purge [*Fastie et al.*, 1973]. These observations are independent evidence that the UVS was performing as designed.

Ground–Based Spectrometry

The first two reports on the sodium exosphere were based on observations just above the sunlit limb. From observations extending 40 km above the limb, *Potter and Morgan* [1988*a*] obtained a subsolar point density, $[N_{Na}](r_0) = 67 \pm 13$ atoms cm^{-3} and a scale height, $H_{Na} = 120 \pm 42$ km, while the subsequent measurement by *Tyler et al.* [1988] obtained $[N_{Na}](r_0) = 57 \pm 20$ atoms cm^{-3} and $H_{Na} = 79 \pm 8$ km (since revised to 75 ±27 km; Sprague, private communication, 1990]. Both assume a simple isobaric exosphere. Potter and Morgan estimated that the full width at half maximum (FWHM) of the sodium line was approximately 42 mA which would correspond to approximately 1100 K if the Na velocity distribution were Maxwellian (in the discovery paper this temperature was incorrectly given as 600 K). Potter and Morgan also reported observations above the lunar poles showing that the Na exosphere extended to the lunar poles with little diminution. Potter and Morgan also studied the K exosphere finding $[N_K](r_0) = 15 \pm 3$ atoms cm^{-3} and $H_K = 90 \pm 20$ km.

The exploration of the vertical extension of the Na atmosphere came quickly. *Potter and Morgan* [1988*b*] reported a series of observations of emission in the Na lines which extended to 1200 km above the bright limb of the Moon. They analyzed these data together with their discovery observations, and obtained a fit with a two component exosphere although they noted that a single large scale height would fit the data as well. If the velocity distribution of sodium were Maxwellian then a single large scale height would lead to a broad line (> 42 mA). One should note here that small changes in FWHM correspond to large temperature variations in the sodium D_2 line; a change from 38 mA to 46 mA FWHM corresponds to a 600 K temperature range.

There is a large difference between the observations of *Tyler et al.* [1988] and *Potter and Morgan* [1988*a*, *b*]. The difference in the observed emission between the two data sets in the D_2 line is almost a factor of 1.5 just above the limb; and, a factor of 3.6, 100 km above the limb. It is of course possible that the sodium exosphere of the Moon is variable.

Derivation of Standard Quantities From Observations

A given atmosphere due to any species will be a mix of accommodated and source atoms. The relative abundances of the two components depend on the average velocity of the newly supplied atoms and the gas–surface accommodation rate. The observed photon flux from scattering is

$$4\pi\mathcal{F} = g\int [N](r)\cdot ds \tag{1}$$

where g is the scattering probability, $[N](r)$ is the number density at r, and ds is the differential element along the line of sight at r. Integration along the line of sight produces different analytic formulations for the two (source and accommodated) components . If we assume the accommodated component dominates and approaches a barometric distribution, the abundance (η_i) at the limb approaches

$$\eta_i(r_0) = [N_i](r_0)\cdot(2\pi\cdot r_0\cdot H_{i0})^{\frac{1}{2}} \tag{2}$$

At the other extreme, if none of the gas is retained and the distribution is coronal, then

$$\eta_i(r_0) = [N_i](r_0)\cdot\pi\cdot r_0 \tag{3}$$

[*Barth*, 1969] where $[N](r_0)$ is the density at the surface. With the exception of H, it has been generally assumed that the atmospheric species are accommodated to the surface temperature. Thus *Fastie et al.* [1973] assumed that the atmosphere was a barometric exosphere with exobase at the surface and at the surface temperature (300 to 400 K). As we shall see below several possible sources of atmospheric constituents should produce at least an initial velocity distribution which is energetic relative to the lunar surface temperature.

Once gas generated by the source processes is accommodated to the surface temperature to form an ambient atmosphere, various loss processes control the steady state population against production. Since the lunar atmosphere is exospheric, loss processes are limited to interaction with solar particles and photons, reactions with the surface, and escape. The relationship of the population to the rate of production of ambient gas can be simply written,

$$S_{ai} = [N_i](r_0)\cdot H_{i0}/\tau_i \tag{4}$$

where $[N_i]\ (r_0)\cdot H_{i0}$ is the vertical abundance of species i, H_{i0} is scale height, S_{ai} is ambient particle source rate (not to be confused with the total source rate, S_i), and τ_i is effective lifetime. Atmospheric lifetimes can vary widely depending on species specific reactions. For a given species, lifetime can also vary strongly depending on whether it is in the sunlit or dark atmosphere. The globally integrated version of (4) may therefore provide lifetimes significantly different from values at specific locations. Some of the source reactions produce product species with kinetic energy above the escape energy so that only a fraction f_a contributes to the ambient atmosphere. Thus the component of the sources described below that provide accommodated atmospheric gas is written

$$S_{ai} = S_i\cdot f_a \tag{5}$$

Sputtering of the Regolith

There is in situ evidence for the action of three vapor producing processes on the Moon: sputtering by solar wind ions, solar photon induced desorption, and impact vaporization following micrometeroid impact. *Potter and Morgan* [1988*b*] argued that two of these processes, impact vaporization and sputtering, taken together can account for the observed sodium exosphere of the Moon. In the present calculations an Na source rate in excess of the requirement in the Potter and Morgan interpretation of the observed data, is obtained. We review this issue below, and argue that the observations actually imply a large source rate. Since oxygen is a significant component of the regolith, these processes will also be a source of atmospheric atomic oxygen. The loss and source reactions controlling the atmospheric species are summarized in Tables 2 and 3. We consider the regolith derived sources here. In the following section we determine the meteoroid and comet derived contributions.

The Physics of Particle and Photon Impact Desorption of Surface and Subsurface Species

Experimental work on photon, electron, and ion interaction with insulator surfaces has revealed basic similarities in the process of desorbing solid state species [see *Tolk et al.*, 1988; *Knotek and Feibelman*, 1979]. Although the reactions can involve complex Auger processes and momentum transfer, desorption of species from the solid state can be described as mainly produced by excitation of dissociative electronic states of the solid molecules which provide sufficient energy to the atomic products to allow diffusion through the subsurface structure. The excitation of the molecular electronic states is accomplished mainly by collisions with low energy secondary electrons generated by the ionization of the subsurface solid by the primary impactor, either photons, electrons, or ions. Direct laboratory experimental evidence for these processes has been obtained for solid amorphous SiO_2 by *Johanessen et al.*, [1976], and *Carrière and Lang* [1977]. *Carrière and Lang* [1977] have obtained quantitative data for dissociative desorption yield, but estimates of yields from the lunar regolith must address the likely change in the yields due to soil maturation. Desorbed silicon atoms tend to undergo low energy chemistry with the surface as the aging process proceeds leading eventually to an oxygen starved surface layer, resulting in an impaired desorption yield. *Carrière and Lang* [1977] report that trace amounts of carbon in the experimental system also have an eventual significant effect in quenching the atomic desorption process.

Proton impact can provide desorption through momentum transfer in addition to the process of electronic excitation and production of secondary electrons. This branch of the desorption process may produce molecular species but the contribution to the total is small. The principal desorption mechanism, dissociative excitation, ends in the production of atomic species [*Carrière and Lang*, 1977]. The physical process described here as the main contributor to

desorption in amorphous silicates is basically different from the sputtering mechanism described by *Johnson* [1989], in which the process is mainly momentum transfer to ground state molecules. In this case the semi empirical formulation for the process involves the molecular ground state binding energy [see *Johnson*, 1989], whereas the electronic dissociative excitation process described above depends on the shape and alignment of repulsive excited states. The difference between these two mechanisms leads to differences primarily in predicted kinetic energies of the desorbed species. If the lunar surface has properties that can be described by the behavior of amorphous silicates, then the major fraction of the desorbed population is expected to have initial kinetic energies below the value required for escape.

TABLE 2. Reaction Probabilities for Lunar Atmospheric Species

	Reaction	(E_h[a]), eV	P, 10^{-6} s^{-1}
(R1)	$h\nu + Na \rightarrow Na^+ + e$	.	16.
(R2)	$h\nu + Na \rightarrow Na + h\nu$ (5893 Å)	.	8.1×10^5
(R3)	$h\nu + K \rightarrow K^+ + e$	.	29.
(R4)	$h\nu + K \rightarrow K + h\nu$ (7670 Å)	.	1.1×10^6
(R5)	$h\nu + O \rightarrow O^+ + e$	.	0.21
(R6)	$H^+ + O \rightarrow O^+ + H$	.	0.2
(R7)	$h\nu + O \rightarrow O + h\nu$ (1304 Å)	.	4.6
(R8)	$(surf)^- + O \rightarrow O^- + (surf)$	.	.
(R9)	$h\nu + OH \rightarrow OH$ (A-X) 3085 Å	.	265.
(R10)	$h\nu + OH \rightarrow O + H$	0.02	18.
(R11)	$h\nu + OH \rightarrow$ (ion product) + e	.	.
(R12)	$H^+ + (surf) \rightarrow OH + (surf)$	.	.
(R13)	$h\nu + H_2O \rightarrow OH + H + h\nu$ (A-X)	.	1.
(R14)	$h\nu + H_2O \rightarrow OH + H$	0.04	10.[b]
(R15)	$h\nu + H_2O \rightarrow H_2 + O$	0.08	1.4
(R16)	$h\nu + H_2O \rightarrow$ (ion product) + e	.	0.4
(R17)	$H^+ + H_2O \rightarrow H_2O^+ + H$	.	4.
(R18)	$h\nu + CO_2 \rightarrow CO + O$	2.0	12.
(R19)	$h\nu + CO \rightarrow O + C$	0.94	0.3

Total ionization probability P($10^{-6}s^{-1}$): Na, 16; K, 29; O, 0.4; H_2O, 4.4. Escape energy (eV): H, 0.03; OH, 0.51; Na, 0.69; O, 0.48; H_2O, 0.54; K, 1.2; C, 0.36; CO, 0.84.

[a] Energy of the heavy product.

[b] For Solar H Lyα, P = 5×10^{-6} s^{-1} at solar maximum. For LISM H Lyα, P = 7×10^{-9} s^{-1}.

TABLE 3. Lunar Atmospheric Globally Averaged Source Rates
$S_i(10^6$ cm^{-2} $s^{-1})$

	Regolith			External		
Species	Ion impact sputtering	Impact vapor	Photon impact	Meteorite	Comet	Small comets
Na	0.024	0.10	0.005	0.02	0.01	0.08
f_a	0.5	0.25[a]	1.0	0.25[a]	0.05	0.10
K	0.0025	0.010	0.0005	0.0014	0.0007	0.006
f_a	0.7	0.25[a]	1.0	0.25[a]	0.05	0.10
H_2O	.	.	.	0.25	6.7	79000.
f_a	.	.	.	0.75	0.05[b]	0.10[b]
O	1.0	.	0.6	.	.	.
f_a	1.0	.	1.0	.	.	.

	S_{ai}[c]	S_{ai}[d]
Na	0.048	0.056
K	0.0051	0.0057
H_2O	0.52	7900.
O	1.6	.
$H_2O \rightarrow O$	0.37	5800.

$S_{ai} = \sum S_i \cdot f_a$ (10^6 cm^{-2} s^{-1})

[a] Retention factors may be severely modified by low energy chemistry. See text.

[b] Retention factors based on scaled down values of *O'Keefe and Ahrens* [1977*a*,*b*]. See text.

[c] Excluding small comets.

[d] Including small comets. Small comet metal content from Frank et al. [1987] [see Wasson and Kyte, 1987].

Sputtering by Solar Wind Ions

The erosion due to sputtering by a flux of incident ions is measured by the yield, Y, which is the number of atoms removed per incident ion [*Sigmund*, 1981]. The yield is well defined only for a monoenergetic beam of ions at normal incidence on the target material. If the target is crystalline, the orientation of the incident beam to the fundamental crystallographic planes should be specified as well. The yield also depends on the exposure history, that is, the dosage of radiation already received. Thus the direct application of laboratory yields to regolith materials exposed for long periods to a large range of ionic species and energies is questionable. On the Moon we have in situ measures of the sputter erosion rate [*McDonnell*, 1977]. The sputter desorption yield for a freshly exposed silicate surface may be as large as 0.4 Å yr^{-1} [*Bilrig et al.*, 1975], but this efficiency decreases rapidly with exposure age to approximately 0.03 Å yr^{-1} for mature surfaces. We use the sputter erosion yield for mature surfaces here to estimate the source rate of regolith species due to sputtering.

Assuming a particle density of 2.7 g cm^{-3} and the average regolith abundances given in Table 1, 0.031 Å yr^{-1} has been converted to atmospheric source flux. The results can easily be scaled for a different regolith abundance of any species. There are abundance variations across the surface of the Moon. The results in Table 1 are very conservative. Using the average yields available in the literature [*McGrath et al.*, 1986], *Morgan et al.* [1989] calculated an average source for sodium which is almost 20 times that given here. These differences between in situ studies and laboratory sputtering measurements are influenced by values of an upper limit to yield typical of data for alkali halides given by *McGrath et al.* [1986]. The sputtering efficiency of silicates is lower and depends on previous dose history. A fresh surface shows a large yield of sodium and other cations, but the yield drops as a sputtered zone a few hundred Å deep is formed at the surface. Since at any time some fraction of the exposed regolith is fresh, the estimates made here for sputtering should be viewed as lower limits. The dominant sputtered species is oxygen based on the experimental evidence discussed above.

Solar Photon Induced Desorption

Research on the desorption of solid atoms from semiconductors and insulators is relatively recent, and quantitative estimates applicable to the regolith are difficult to make because of a general marked dependence on the microstructure of the surface. In general photons are absorbed in the solid by exciting the electronic structure, which ends in various branches involving ionization, ionization–excitation, and excitation of neutral states. Some of these branches result in dissociation and subsequent diffusive loss from the solid [see *Tolk et al.*, 1988; *Husinsky et al.*, 1988; *Tolk and Larchuk*, 1984; *Knotek et al.*, 1979; *Knotek and Feibelman*, 1978; *Carrière and Lang*, 1977]. Direct experimentation on lunar surface fines [*Feuerbacher et al.*, 1972] has produced quantitative measurements of the yield of electrons from reaction with photons, but there are no results for desorption of neutral species. However, based on the physics of the desorption process discussed above, the appearance of electron emission implies the production of desorbed neutral atomic species. The efficiency for the desorption of neutrals is significantly larger than for ions [*Tolk et al.*, 1988]. As with other sputtering processes, the efficiency is reduced for radiation damaged surfaces, and the photon absorption process must be near the surface to be effective. Typical yields for desorption are $10^{-5} - 10^{-6}$ [*Knotek and Feibelman*, 1979], and we conservatively take a value 10^{-6} for amorphous silicates under the solar flux. The calculated rates are given in Table 3.

Impact Derived Species

Impact derived H_2O and other volatiles may be separated into three sources: micrometeoroids; comets; and small comets as proposed by *Frank et al.* [1986]. Since all of these processes involve hypervelocity impact on the surface of the Moon, we must determine the fraction of volatiles to survive as atmospheric particles. In what follows H_2O, Na, and K will be considered in detail.

Vapor from Micrometeoroid Impact

The mean impact velocity of the incoming meteoroids is 15.8 km s^{-1} so that the bulk of the infalling meteoroid population strike the surface with velocities which are several times the bulk speed of sound in most meteoroid materials. As the impact proceeds, a strong shock passes through the entire projectile, and the shock reflects from the rear boundary forward into the volume of the meteoroid [*Ahrens and O'Keefe*, 1972]. Under these conditions, vaporization, melting, or at minimum, shock heating and shock induced structural change occur throughout the projectile. Loss of H_2O in particular extends to the portions of the infalling meteoroid which survive the impact as melt and as shocked solid [*Boslough et al.*, 1980; *Tyburczy et al.*, 1986; *Tyburczy and Ahrens*, 1988]. Complementing this is the well documented dearth of H_2O in the lunar regolith.

The effects are just as pronounced in the regolith; vaporization and melt production in particular occur at the point of impact. The regolith lacks a large population of volatile species, and the principal contribution to the atmosphere will come from the fraction of the regolith which is vaporized in the impact. The initial vapor cloud produced by shock vaporization of the regolith is not in thermal equilibrium. However, the spectrum of the impact flash (incandescent gas formed at impact) observed by *Eichhorn* [1978] could be fitted with a Planck function. The temperature associated with the Planck function varied from 2500 K to 5000 K being dependent on impactor/target characteristics. The approach to thermal equilibrium in the hot vapor must therefore be quite rapid. If we assume a temperature of 2500 K, then under equilibrium conditions only sodium and potassium would be present in the vapor as atomic sodium and potassium [*Fegley and Lewis*, 1980]. The estimated source rates for Na and K [*Morgan et al.*, 1989] are given in Table 3. There is both in situ evidence for loss of Na and K in the agglutinitic glasses in the lunar regolith [*Gibson et al.*, 1975] and laboratory evidence for the loss of Na and K (together with some silica loss) from impact melts [*Florenskiy et al.*, 1977]. The early stages of vapor production in an impact are not in strict thermal equilibrium with one temperature, and small populations of other metallic neutrals and metallic ions may be present. But in general these elements remain bound in high molecular weight silicate molecules which should not contribute directly to the atmosphere.

The main volatile species of interest in the infalling meteoroid material is H_2O. While other volatile species are

almost certainly present in the meteoroid population, their abundances are poorly known and these species are likely to be minor constituents (sulfur being a prominent exception). *Morgan et al.* [1989] calculate that 57.6 g s^{-1} of meteoritic material impacts the Moon, and the composition of the bulk of this material is probably closer to the composition of the IDPs than of the meteorites. Systematic compositional studies of the IDPs are now available [*Schramm et al.*, 1989], but there are generally only indirect measures of water content. However, these indirect measures run as high as 7% by mass for one large class of IDPs. Here we shall assume that the abundance of water is 5% H_2O by mass (M. Zolensky, private communication, 1988). Thus, the meteoritic H_2O source amounts to

$$S_{H_2O} = 0.75 \times 10^{-17} \text{g cm}^{-2}\text{s}^{-1} = 2.5 \times 10^{+5} \text{ molecules cm}^{-2}\text{s}^{-1} \quad (6)$$

Arnold [1979] calculated a source rate for H_2O a factor of 5 less than (6), but he assumed less than a quarter of the incoming flux as we used above and an H_2O mass fraction of 3%. The factor of 5 difference between the result of *Arnold* [1979] and the present work is indicative of the range of uncertainty in these calculations, particularly the meteorite flux at 1 AU [*Tuncel and Zoller*, 1987].

Prompt Loss Following Impact

Some of the vapor produced by impact may be promptly lost from the Moon. There are several ways to lose the source H_2O and alkali atoms promptly. First, the dissociation energy of water is 5.1 eV and impact flash spectra of meteoroid projectiles containing Ca (ionization potential (IP), 6.1 ev) obtained in the laboratory show emission in the Ca II H and K lines (B. G. Cour–Palais, private communication, 1988). Much of the H_2O in the prompt vapor component may be dissociated into OH and H. However impact flash spectra sample only the initial phase of the vapor cloud formation, and provided the OH is not lost by escape, there is no diminution of the supply to the observable daughter molecules, OH and O.

The IP of Na and K is 5.1 eV, and 4.3 eV, respectively. Since ions of Ca and Al (IP = 6.0 eV) are formed in high velocity impacts, we can only assume that some Na and K are ionized as well. An ion has at least 50% probability of loss to the solar wind. However the ionized fraction is likely to be small.

Much of the vapor formed in the early stages of the impact will leave the Moon. The more refractory species which should be concentrated in the hottest fraction of the vapor derived from the impact will be preferentially lost. Two high velocity vapor components may be present. In all hypervelocity impacts there is an approximately spherical rapidly expanding hot vapor cloud formed at impact. In oblique impacts, jets of gas and other debris have large lateral velocities [*Schultz*, 1987]. The range of expansion velocities present in the expanding spherical cloud can be calculated to a reasonable approximation by treating the expansion as a sudden isentropic expansion of a dense hot cloud of gas into a vacuum. For initial conditions appropriate to micrometeoroid impact one finds that most of the gas in this expanding cloud is blown off planet (Appendix A). For example, if the initial temperature of the gas cloud is 2500 K, the velocities range from 4.65 to 1.55 km s^{-1}. If the gas is evenly distributed over the entire range of velocities, then only a quarter of the gas is below escape velocity. The more refractory elements (refractory relative to such volatiles as water) like Na and K are likely to be confined to the hotter portions of the vapor produced, and are thus likely to have retention fractions on the order of 0.25. Retention factors become a more complex issue if energetic atoms impacting the surface undergo low energy chemical reactions with associated activation energies larger than the escape magnitude as discussed below in relation to the observed atmospheric distribution of Na.

However, volatile species (H_2O, CO, CO_2, and SO_2) will be derived from all portions of the projectile, and the bulk of the volatile loss will be from those volumes of the meteorite that are not completely vaporized in the early phases of the impact. In addition the meteoroid material as a whole continues downward well into the impact, and most of the meteoroid material is not lost from the Moon on impact [*Ahrens and O'Keefe*, 1972, 1977; *O'Keefe and Ahrens*, 1976, 1977*a*,*b*]. The fact that the very volatile fractions are derived from the meteoroid and characterized by a large range of temperatures (5000 K to ambient) makes their deposition after impact different from less volatile species, Na and K, that are predominantly derived from the regolith. Here a simple and conservative assumption will be made: namely that a quarter of the H_2O is lost to the Moon immediately upon impact.

Cometary Impacts

Comets and small cometlike objects[*Frank et al.*, 1986] differ from the meteoroids in several respects. First, the water content of both is much larger in these objects than in the the meteoroid population. Second, a larger fraction of the incoming material is likely to be lost to the Moon on impact than is the case for the micrometeoroid population. We turn first to comets. *Ip and Fernandez* [1988] estimate that the Earth has accreted 2.8 × 10^{20} g of cometary material in the last 4 b.y.. Scaled to the Moon, we have 0.21 × 10^{20} g of cometary material in 4 b.y. or

$$S_{H_2O} = 2 \times 10^{-16} \text{g cm}^{-2}\text{s}^{-1} \quad (7)$$

if half of the mass is water. To state the input as a constant source is somewhat misleading because input of the material is episodic, major accretions followed by long periods of drought. But cometary impacts can initiate formation of frost deposition on permanently shadowed regolith. Ip and Fernandez obtained 7 × 10^{16} g for the average mass of the incoming comet population. It follows that the average time between impacts is 13.3 million years. The actual sequence of impacts is quite uneven however, and should resemble the models of the cometary water input to the atmosphere of Venus by *Grinspoon and Lewis* [1988]. The mean source rates are given in Table 3.

The periodic comets differ from both the meteoroids and from the *Frank et al.* [1986] small comets, being intermediate in density and composition between the meteoroid population (in which H_2O is a minor constituent in an assemblage of silicate minerals as water of hydration) and the Frank et al. small comets, which are porous and composed almost entirely of H_2O. Infalling comets impact at infrequent intervals, and they can only be an important contributor to the present exosphere if there is a storage mechanism like frost deposits. However we will consider the fraction of the

cometary material likely to be retained on the planet initially here. As an archetype, one may adopt an inhomogeneous, Halleylike composite object with average nucleus density [*Keller et al.*, 1987] , 0.4-0.6 g cm^{-3}. The composition may be approximately 50% water, 30% CO_2 and other volatiles, and 20% refractory materials. The range of impact velocities is approximately 30-100 km s^{-1}. Under these conditions, the periodic comets can be expected to contribute only a fraction of their material to the surface.

O'Keefe and Ahrens [1982] followed the impact of a series of low density (1 g cm^{-3} to 0.01 g cm^{-3}) ice projectiles impacting a silicate regolith at normal incidence. Although none of their assumed cases corresponds exactly to realistic cometary impact, the calculations provide a framework in which to discuss the likely results of such impacts. First, these objects may be expected to produce a net erosion from the surface [*O'Keefe and Ahrens*, 1977*a,b*, 1982]; that is the mass of material, both regolith and cometary, blown directly away from the Moon is larger than the mass of the incoming body. This does not mean that all of the cometary material is lost, for much of the ejected matter is derived from the regolith. The projectile (the comet nucleus) vaporizes early in the impact; the velocity flow field of the projectile derived material is critically dependent on the impact velocity, the density, and the heat of vaporization of the projectile. However, one expects a large fraction to be removed. The chemical interactions of the cloud of superheated water vapor with the regolith were not included in the calculations of O'Keefe and Ahrens and it is these processes which may be the most significant retaining mechanism. The impact of a heterogenous projectile (coma plus a composite nucleus) might leave almost any fraction of the volatile content depending on the impact conditions, the fraction of hydrated silicaceous material, the compaction of the volatile material, and the fraction of the water which reacts chemically with the regolith and regolith ejecta. We shall simply assume that on average a quarter of the incident water is retained, and note that there is a very large uncertainty in this number.

The Frank et al. Small Comets

Frank et al. [1986] proposed a population of small cometlike objects incident on the top of the Earth atmosphere with velocities from 16 to 20 km s^{-1}. The flux of small comet material onto the surface of the Moon should be 1.4 $\times 10^3$ kg s^{-1}. If we assume that most of this is H_2O, we have

$$S_{H_2O} = 3.7 \times 10^{-12} \text{g cm}^{-2}\text{s}^{-1} = 1.2 \times 10^{11} \text{molecules cm}^{-2}\text{s}^{-1} \quad (8)$$

This is quite a steady supply as well. We calculate (including gravitational focussing) using the *Frank et al.* [1986] rate of 20 per min on the Earth, approximately 52 collisions by small comets with the surface of the Moon every hour, each of which should provide a pulse of $\approx 10^{30}$ molecules to the Moon. *Dessler* [1991] obtained a similar rate, while Davis [1986] neglecting gravitational focussing obtained 90 collisions per hour. *Donahue et al.* [1987] [cf. *Hall and Shemansky*], 1988*a*] and many others [see *Dessler*, 1991] argue against a quantity of this magnitude. We have separated this source from the total in Table 3 because of the enormous impact it has on consideration of the physical limits of the lunar atmospheric system, as discussed below.

The prompt losses associated with the small comets are more easily estimated since they are assumed to be almost entirely water. These comets have a density of 0.1 g cm^{-3} water ice and impact at 15 km s^{-1}, corresponding to the calculations shown in Figures 5 and 16 of O'Keefe and Ahrens [1982]. This particular case stands in sharp distinction to both water and silicate projectiles at other densities [*O'Keefe and Ahrens*, 1982, Figure 20] in that a large fraction of the projectile energy (more than 50%) remains in the projectile material well into the impact (the calculations do not extend to infinite time). By comparison similar calculations by the same authors predict that less than 10% of the initial projectile energy remains with the projectile material following impact in the case of a 1 g cm^{-3} ice projectile.

According to *O'Keefe and Ahrens* [1982] the mass of material to escape relative to the mass of the projectile is close to 1 for the impact of a small comet with density 0.1 g cm^{-3} with both regolith and cometary mass contributing. For a 15 km s^{-1} impact of a 0.1 g cm^{-3} impactor, the fraction of the initial energy partitioned into regolith motion is 0.12 while 0.38 of the initial energy is partitioned into kinetic energy of the small comet material. This implies that the retention factor for the small comet material should be $f_a = 0.25$. In order to insure that a conservative estimate is made we apply a value of $f_{aH_2O} = 0.1$ in Table 3. This estimate is based entirely on the dynamics of the impact process, and does not include possible subsequent physical chemistry of the hot atomic and molecular species impacting the surface. If some fraction of the hot H_2O undergoes chemical scale adsorption the retention factor could be larger than the value derived from the *O'Keefe and Ahrens* [1982] calculations. We have found it necessary to invoke surface physical chemistry for hot Na impacts in order to explain observationally determined $f_{aNa} \sim 0.01$. The effect of an analogous reaction at the surface for H_2O would produce a very different result, since the dominant subsequent desorption reactions involve dissociation to OH + H as discussed above and below, with kinetic energies that are probably below the escape value for OH, particularly if H_2O electronic structure is the dominant factor as expected. The retained H_2O is mainly converted to OH, with subsequent photoexcitation of the OH (A – X) transition near 3085 Å . The estimated OH (A – X) (0,0) band brightness based on $f_{aH_2O} = 0.1$ is therefore 750 kR at the limb whether or not surface chemistry is assumed to be involved. If chemistry at the surface is in fact involved at significant rates, the retention factor used here may be exceedingly conservative in respect to the small comet source, and the brightness of the OH band could be in the range of several MR. It is always possible that some physical resonance that we are currently not aware of may negate the result predicted here. If the lifetime of the ambient atmosphere were significantly shortened by an analogous reaction to (R8) (Table 2) as discussed below, the emission brightness would be proportionally reduced. However, if the OH lifetime were shortened to 1 hour by such a process, the OH(3085 Å) emission brightness calculated above for $f_{aH_2O} = 0.1$ would only be reduced to 50 kR. A factor of ~ 500 is required to reduce the predicted emission in the OH(A – X)(0,0) band to 100 R, the order of the upper limit imposed by observation. However, the escaping component of the gas also contributes to the expected emission.

We show calculations of the contribution of the escaping gas to emission in Appendix B. As noted earlier, the expressions in Appendix A agree with available laboratory measurements of the expansion velocity of prompt vapor clouds formed during high velocity impacts. The expansion velocities have also been calculated for the impact of a projectile composed of H_2O ice, for each of three assumptions regarding the initial composition of the vapor. Two of these are asymptotic extremes that are physically unlikely but carried out here to illustrate the observable effect. The assumed vapor products are: (1) H_2O, (2) OH + H, and (3) O + H + H. In each case (Appendix B) the predicted expansion velocities are as large as those calculated for the expansion of the prompt vapor cloud from meteoroid impact.

The expected emission in OH and O transitions in the escaping gas is estimated in Appendix B, for the three cases described above. The predicted brightness for OH 3085 Å is 0.3 kR for case 1, and 3. kR for case 2 at an altitude of 10 R_M. The predicted O 1304 Å brightness above the bright limb is 1. R, 18. R, and 700 R, for the three cases (Table B2). There is a reported upper limit of 30 R in the OH transition [*Hall and Shemansky*, 1988*b*] 3 to 20 R_M above the limb(IUE LWP exposure of 3 hours on 1988 day of year 219), and as discussed in an earlier section there is an < 0.1 R upper limit to O 1304 Å emission at the limb (to be compared to half the predicted brightness given above). The OH and O distributions are very extended (Table B2). However, OH emission has never been detected by the IUE satellite in the interplanetary medium or above the lunar limb, and the Apollo UVS did not detect O, in the Earth–Moon environment.

The composition of the coronal source is likely to be dominated by case 2, for small comet impact with the surface. The fraction of initial energy partitioned into internal energy of the low density comet is 0.25 according to the O'Keefe and Ahrens calculations. This translates to 5.8 eV per molecule, the same order as the H_2O dissociation energy, 5.4 eV, and serves as an indicator that in the range of temperatures achieved in the impact there is sufficient energy for dissociation of most of the H_2O. Since H_2O is not a homonuclear vibrator, the delivery of energy to the dissociation process is directly competitive as a rate process with other momentum transfer effects, indicating that on a qualitative basis a substantial fraction of the internal energy will be delivered to dissociation to OH + H. The exact fractionation will depend on the temperature history of the gas; vibration times are extremely short relative to the scale of the impact (fundamental vibrational period 2. $\times 10^{-14}$ s), and vibrational energy transfer is expected to track the impact dynamics. The lifetime of an H_2O molecule against dissociation in a collisional regime at 2000 K is of order 5 ms, and rapidly shortens exponentially with increased temperature. The expansion velocity of the gas (Appendix B) is the temperature equivalent of order 15000 K. Individual H_2O molecules impacting the lunar surface at 15 eV will certainly dissociate, and the only major uncertainty is partitioning of absorbed, adsorbed, and scattered OH and atomic particles, which ultimately become part of a stabilized atmospheric source. H_2O has not been detected in analyses of the lunar regolith. However, in any of the three asymptotic cases the predicted rate for small comet influx is so high that calculated emissions far exceed observed limits. Until there is some explanation for the disagreement with the emission data, we propose to separate the small comet source from other lunar exosphere and coronal sources, in the consideration of minimum rates.

Cold Traps as Atmospheric Sinks

The ambient species can be lost by photoionization, photodissociation, charge–exchange, and by Jeans escape. Cold traps in or on the surface can collect species, but these sinks are local, and if sufficient time for equilibration is available the gas will return to the atmosphere at the same rate as the adsorption or absorption process. The issue in this case is the lifetime of the captured gas. We propose below an additional loss mechanism that may be mainly specialized to atomic oxygen, in which reaction with the negatively charged darkside surface may result in loss through electron capture to form O^-. The photo– dissociation and photoionization rates at 1 AU for H_2O, OH, CO_2, and CO are known and tabulated in Table 2. The photoionization rates and the charge exchange rates due to solar wind protons are also known, and are much larger than the Jeans escape rate for accommodated species. Long lived trapping by the surface and surface catalyzed losses are more difficult to assess. Here we consider surface trapping and in the following section we examine surface catalyzed losses.

If a permanently shadowed area is to form an effective atmospheric sink, the adsorption lifetime of the gas must be long enough to be comparable to the regolith gardening period as a process limiting the desorption of the gas. The cold trap must be in disequilibrium with the atmosphere in order to be a net sink, requiring exceedingly long adsorption or absorption lifetimes. The sink must defeat outward diffusion and the process of sputtering by particle or photon impact. As we shall see below sodium and oxygen have relatively short physical adsorption time constants on bare silicate surfaces. Trapping of these species by water ice in the permanently shadowed regions [*Watson et al.*, 1961] would be a much more effective mechanism. We shall examine the possible modes of water frost or ice deposition and whether such a deposit is a sink or a net source for exospheric species.

The entrapment of gas at the solid requires special conditions if the lifetime of the trapped gas is to be considered long enough to constitute a sink. For adsorption or even absorption to work in this way requires very low temperatures. Loss may be accomplished through chemistry such as interaction of OH with reduced Fe, but this requires reactants with sufficient energy to overcome the activation energy for the process. However, in a chemical reaction at or very near the surface, the lifetime of the compound may in general be too short to be considered as a real sink process. Such processes may in many cases simply stabilize source rates rather than constitute loss processes. There is very little H_2O in the lunar regolith so surface trapping of H_2O on most of the lunar surface must be a secondary process at best. Permanently shadowed regions cover perhaps 0.5% of the lunar surface and are concentrated in the lunar polar regions. To gauge the effect of a frost on the atmospheric abundance of H_2O and other volatiles we must examine the likely temperatures to be found in these regions, the stability criterion for the frosts, and the likelihood of initial formation.

Surface Temperatures

The heat flux from the deep interior of the Moon is 1.8 $\times$ 10^{-6} W cm^{-2} [*Langseth et al.*, 1976]. The regolith is an effective thermal insulator, so that lateral heat flow from nearby sunlit areas is unlikely to supply significant amounts of thermal energy to regions more than a few meters across. The flux of solar wind protons is 4.3 $\times$ 10^8 protons cm^{-2} s^{-1}. If all the energy of this flux is available to heat the regolith (0.84 keV/proton), the power that must be dissipated is 0.58 $\times$ 10^{-7} W cm^{-2}. This flux of heat may be considered an upper limit for the contribution by energetic particles [*Lanzerotti et al.*, 1981]. Next we must consider the possible heating by the interplanetary H Lyα emission which is approximately 0.5 – 1. kR. Total absorption of these photons (at 10.4 eV per photon) leads to 1.6 $\times$ 10^{-11} W cm^{-2}. If these three alone heat the surface, the surface temperature would be only 26 K. In most cases the permanently shadowed areas have less than a 2π steradian field to deep space. Generally, some portion of the field of view will be sunlit during part of each lunation. If the average temperature of the sunlit areas is 300 K and they fill 1% of the field of view, the effective flux from this source alone will reach 4.6 $\times$ 10^{-4} W cm^{-2} s^{-1} if the permanently shadowed area is a perfect absorbing surface. Each site will be unique, and the sunlit portion of the field of view should vary throughout the lunation. Taken together, these considerations suggest that the lunar surface temperature, T_{psr}, of permanently shadowed regions is 26 K(total shadow) < T_{psr} < 95 K (sunlit surfaces in field of view). The upper limit can be compared to the measured minimum temperatures at high latitudes via ground–based measurements as low as 84 K due to *Wendell and Low* [1970]. Most triatomic species should be effectively adsorbed at these temperatures. The basic question is, what processes limit the lifetime of the adsorbed gas?

The Regolith as a Sink for Volatiles

Atomic species do not adsorb as readily on cold silicate surfaces. If we take the well depth for physical adsorption of O on a quartz surface as calculated by D. E. Shemansky and J. Kunc, (manuscript 1988) [see *Hunten et al.*, 1988], D_0 (O – SiO_2) = 837 K, the lifetime on a surface at T_s = 26 K is τ (O – SiO_2) = 25 s. The surface at this temperature would therefore not be considered a trap for atomic oxygen under ideal conditions. In contrast, a sodium atom with D_0 (Na – SiO_2) = 2900 K [Shemansky and Kunc, manuscript, 1988; see *Hunten et al.*, 1988] will have τ (Na – SiO_2) $\approx$ 10^{28} years for T_s = 26 K. The limiting factor for the lifetime of Na on the cold surface would therefore certainly not be thermal capacity of the surface, but probably photodesorption, photoionization and particle sputtering. The flux of H Lyα onto the surface from the very local interstellar medium (VLISM) is $2\pi\mathcal{F} \approx 5 \times 10^8$ ph cm^{-2} s^{-1}. If the cross section for momentum transfer is 2 barns, the desorption probability is of the order of 10^{-15} s^{-1}, or τ_d = 3 $\times$ 10^7 years. The photoionization process may also effectively act as a desorption reaction depending on the nature of the coupling of the ion produced with the solid. The cross–section for photoionization of Na is σ_i = 0.16 Mb for H Lyα, which if effective for desorption would limit the lifetime to $\tau \approx 400$ years. If scattered solar radiation has access to the shadowed surface through scattering from the rim of the structure, the lifetime could be shortened further.

Stability of Frost in the Permanently Shadowed Regions

The formation of H_2O ice in permanently shadowed regions of the Moon has been considered earlier by *Arnold* [1979] and later by *Lanzerotti et al.* [1981]. The main loss process for the ice considered in these works was sputtering by ions of solar origin. *Lanzerotti et al.* [1981] used experimental erosion rates to arrive at the conclusion that the formation of ice was unlikely. We shall reexamine the erosion processes below using currently available data on the vapor pressure of amorphous ice, the loss due to sputtering, and the effect of UV radiation from the VLISM.

The vapor pressure of amorphous H_2O ice (I_{as}) has been measured at low temperature by *Kouchi* [1987]. The temperature dependence of I_{as} vapor pressure (P_v) has a complex dependence on condensation temperature and rates. We choose one of the higher vapor pressure curves obtained by Kouchi [1987] to calculate the limiting factors. Values of P_v below T = 118 K require an extrapolation, which we have developed using a standard rate equation with a negative entropy of activation. A vaporization flux equated to the globally averaged source flux in Table 3 (5.2 $\times$ 10^5 cm^{-2} s^{-1}) corresponds to a temperature T_s = 67 K. The mean lifetime of the adsorbed H_2O is about 30 years at this temperature. The temperature requirement for formation of a net sink is therefore rather stringent. However, the limiting factor in fact is not the temperature of the surface in this case. *Lanzerotti et al.* [1981] estimated an erosion rate of 10^7 cm^{-2} s^{-1} from solar origin ions. This value is optimistically large because of the experimental surface condition [*Hapke*, 1986], but it nevertheless may be a serious loss factor for adsorbed H_2O. Another loss process not previously considered is the fact that permanently shadowed regions are exposed to the flux of H Lyα from the VLISM. H_2O in vapor form is dissociated by H Lyα with significant exothermicity [*Wu and Judge*, 1988]. Since the process is not resonant [see *Wu and Judge*, 1988], the cross section is not expected to be significantly different for an adsorbed molecule. The lifetime for an adsorbed H_2O exposed to a 500 R VLISM H Lyα flux is limited to 4 years (monolayer desorption rate 7 $\times$ 10^6 cm^{-2} s^{-1}; see Table 2 for rate quantities). This appears to be the rate limiting process and it is very unlikely that an H_2O cold trap sink could develop from the continuous supply of water due to infalling meteoroids. The rates are high enough to prevent formation of a monolayer of H_2O, given the present quantities in Tables 2 and 3, if we assume the source is not strongly episodic.

Survival of Episodic Water Deposits

The steady accretion of H_2O to the Moon from meteoroid impact does not lead to the deposition of ice, but the episodic deposition of large volumes of water by impacting comets introduces a basically different condition that needs to be considered. From an earlier section we have an average comet mass of 7 $\times$ 10^{16} g and an average interval between impacts of 13.3 million years. At least half of this average mass should be water. To be trapped in permanently shadowed regions, the water molecules must, first, remain on the Moon after impact and, second, remain in the atmosphere for a time long enough to encounter the cold trap. Of these, the first is a more stringent test, for much of the cometary mass should be lost to the Moon on impact at the expected large intersection velocities. As it is impossible to

estimate the fraction exactly and unlikely that all the water is lost initially, we shall make what we believe to be a conservative assumption; namely, that only 1 molecule in 20 reaches the permanently shadowed regions and is trapped. This amounts to 1.8×10^{15} g of water, enough to cover the estimated area of permanently shadowed region mentioned above to a depth of 1 cm in ice.

As we have seen, the destruction of water by LISM H Lyα dominates all other loss processes and proceeds at the rate of 7×10^{-8} mm yr^{-1}. The rate of creation of new regolith is 1 to 2×10^{-6} mm yr^{-1} [*Quaide and Overbeck*, 1975]. The rate of creation of new regolith is noted here because this material is deposited preferentially on top of existing regolith. It is thus a measure of the rate at which burial of the deposit will take place. Regolith processes are not uniform, and gardening will eventually destroy volatile surface deposits which are not buried, but on balance the net effect of a 1 cm deposit of water ice in the permanently shadowed regions would be the burial of some fraction of it after a few million years. Burial is an effective process for removing material from the effects of gardening. Only a small layer of regolith is required to reduce losses by LISM H Lyα, and by sputtering. Burial will also reduce the peak temperature of the ice, lowering thermal desorption losses.

While the mean interval between impacts is 13 million years and the average mass is as noted above, the actual implacement history is likely to be quite uneven. A core tube driven into a permanently shadowed region would reveal an uneven pattern of alternating horizons of ice and regolith.

Condensates as a Source of Exospheric Materials.

Deposits of water ice, and by inference, other ices are not likely to be sinks for the steady–state (away from comet impacts) lunar exosphere, but they may be local sources. Burial of episodic deposits should greatly reduce the rate of loss of water and other condensates from the permanently shadowed regions, but not prevent it entirely. A local loss rate of 10^6 molecules cm^{-2} s^{-1} (global average; 5×10^3 cm^{-2} s^{-1}) corresponds to 10^{-8} mm yr^{-1} which is well below the rate at which comets would appear to input water to the permanently shadowed regions over time scales of 100 million years or more. Yet this would correspond to a source of water which is locally almost an order of magnitude larger than that due to infalling micrometeoroids. If we assume that most of the desorption is due to LISM H Lyα, the frosts provide a localized source of OH that may produce measurable latitudinal differences in zenith column.

Relating Volatile Sources to Observed Species

The most abundant sputter product (Table 1) is O. Incoming meteoroids may provide H_2O and CO_2, but neither should be present in the night atmosphere (sampled during Apollo 17). These two triatomic molecules do not possess strong resonance fluorescence lines in the vacuum UV or visible; their photodissociation products do. The possible daughters are OH, H_2, O, H, and CO. A large fraction of the CO_2 dissociation products have escape velocity (see Table 2). Of the possible species from either process, O, for which there is an upper limit (due to *Fastie et al.*, 1973) and OH (upper limit due to *Hall and Shemansky*, 1988*b*) may form an exosphere. Sodium is also included. We consider each below.

Oxygen Exosphere

The upper limit on accommodated atomic oxygen density based on the *Fastie et al.* [1973] experiment is

$$N_O < 5 \times 10^2 \text{ cm}^{-3} \quad (9)$$

This value is based on a new analysis of the UVS data by P. D. Feldman [private communication 1990]. The source rate as indicated above is

$$S_{aOX} < 2.5 \times 10^3 \text{ cm}^{-2}\text{s}^{-1} \quad (10)$$

assuming that the loss rate is determined by photoionization and charge exchange (reactions (R5), (R6), Table 2).

The LACE experiment may place an even lower limit on the source. The physical potential interaction of atomic oxygen with silicates is not deep enough to provide significant adsorption at a surface temperature of 100 K. In the absence of a nightside sink the ratio of the subsolar density to the antisolar density should be inversely proportional to the 5/2 power of the ratio of the subsolar point temperature to the antisolar point temperature. Given a subsolar temperature of 400 K and antisolar temperature of 100 K, the antisolar subsolar ratio should be 32. The LACE experiment should have detected a mass 16 species with an antisolar abundance of > 1600 atoms cm^{-3}. The corresponding subsolar point density is 50 atoms cm^{-3}. This argument is not valid if there is a significant sink on the darkside.

Table 3 shows the estimated atmospheric source rates calculated according to the discussion above. Neglecting those components of the source species that are immediately lost to the atmosphere, the atomic oxygen atmospheric source rate is predicted to be

$$S_{aOX} = S_{aO} + N_{OH} \cdot H_{OH} \cdot P_{10} + N_{H_2O} \cdot H_{H_2O} \cdot P_{15} \quad (11)$$

where P_i is the probability for reaction (Ri) (Table 2), S_{aO} is the rate for direct production of atomic oxygen, and S_{aOX} is the rate including subsequent chemistry. Table 3 gives a value

$$S_{aOX} = 2. \times 10^6 \text{ cm}^{-2}\text{s}^{-1} \quad (12)$$

excluding the small comet source. The inclusion of the small comets would raise the value of S_{aOX} by 3 orders of magnitude. The value given above in (12) is a factor of 1000 larger than the upper limit based on the *Fastie et al.* [1973] measurement (see (10)), and 4000 larger than inference from the LACE. The inclusion of the small comets produces a rate 3×10^6 times larger than the spectroscopically determined upper limit. The source rate implied by this latter class of objects presents a serious conflict with observation. *Dessler* [1991] in an extensive review of the small comets has reached a similar conclusion. This issue will be discussed further below, but we propose to examine the limits of the lunar atmosphere using conservative rate estimates by excluding the estimated small comet source.

The apparent excess in the predicted source rate for O relative to inference from observation and known loss processes has a limited number of possible explanations. An excess in the estimation of the source rate is doubtful, since our calculations are biased toward low rates of the possible sources. The loss processes considered in the above calculation were restricted to charge exchange and photoionization (R5, R6 Table 2), limiting the atmospheric lifetime to 28

days. In order for the observed upper limit on oxygen abundance to be compatible with the calculated source rate, the atmospheric lifetime would have to be reduced to the order of 1 hour. An effective lifetime this short can be obtained in two ways. First, a short transport time to the dark hemisphere of this order may be established if the O atoms were energetically in excess of the surface temperature. If a loss mechanism were present with sufficient efficiency in reactions on the dark surface, the apparent deficiency of oxygen could then be explained. Second, if a major component or components of the source produced a large fraction of the reactant products at energies above the value for escape ($f_{aO} << 1.$), the predicted ambient atmospheric content would be reduced. There is a mechanism for the first loss process as mentioned above, and to be discussed below. The second process may be operative to a relatively small degree, but the component derived from photon stimulated desorption is near threshold, unless the dissociation reaction occurs at the top surface layer.

Sodium Exosphere

The observed sodium in the lunar atmosphere requires a source rate of

$$S_{aNa} = N_{Na} \cdot H_{Na} \cdot P_1 = 0.8 \times 10^4 \text{ cm}^{-2}\text{s}^{-1} \quad (13)$$

from the data in Table 2, if we assume that loss is confined to photoionization. The predicted source rate given in Table 3 is,

$$S_{aNa} = 4.7 \times 10^4 \text{ cm}^{-2}\text{s}^{-1} \quad (14)$$

approximately a factor of 6 larger than the loss rate based on the assumption in (13). Impact vaporization provides approximately 60% of the sodium in this calculation. However, we note a critical issue raised by the *Potter and Morgan* [1988*b*] observations which show a very strong component of Na in an extensive distribution above the limb, and we conclude below that loss rates are actually much higher and limited by escape rather than photoionization. Our analysis of the *Potter and Morgan* [1988*b*] data in fact indicates loss rates that exceed the total value of S_{Na} (1.6×10^5 cm^{-2} s^{-1}) obtained from Table 3.

OH Exosphere

There are no observations at the OH resonance lines comparable to the observations of the O 1304 Å line made by Fastie et al. [1973], but the g value of the OH transition near 3085 Å is 2 orders of magnitude larger than the g value for O 1304 Å (Table 2). As this wavelength region has been observed with the IUE satellite[*Hall and Shemansky*, 1988*b*], the likely observable flux will be examined. The OH source in the present calculation is limited to the quantity derived from the photolysis of H_2O. The dissociation of H_2O to form OH ((R14), Table 2) does not have sufficient excess energy to allow escape of the OH component (Table 2), although there is sufficient energy for chemical reaction at the surface, or insertion in the subsurface at a suitable site. However adsorbed OH will be desorbed and dissociated in a relatively short period by interaction with solar photons. If we assume that the OH produced by photolysis of H_2O ends in accommodated atmospheric gas, the vertical abundance, controlled by the reactions listed in Table 2 and the source rates given in Table 3, is given by

$$N_{OH} \cdot H_{aOH} = S_{aH_2O} \cdot P_{14} \cdot ((P_{10} + P_{11}) \cdot \sum_{13}^{17} P_i)^{-1} \quad (15)$$

The evaluation of (15) gives a value

$$N_{OH} \cdot H_{aOH} = 1.8 \times 10^{10} \text{cm}^{-2} \quad (16)$$

For accommodated OH the scale height $H_{aOH}(0) = 102$ km ($T = 340$ K). The predicted brightness of the OH (A − X) (0,0) band in solar fluorescence is then given by

$$I_{OH}(3085) = \eta_{aOH} \cdot g_{OH}(3085) \cdot 1. \times 10^{-6} = 50 \text{ R} \quad (17)$$

Darkside physical chemistry similar to that proposed for oxygen would reduce the predicted value in (17). Although appropriate IUE observations have been made for limiting coronal OH abundance [*Hall and Shemansky*, 1988*b*; see above discussion in "Frank et al. small comets" and Appendix B) it is doubtful that the IUE satellite can be used to set limits on an accommodated OH atmosphere at the magnitude given by (17).

Discussion

Atmospheric Metals

According to the present calculations, most of the atmospheric sodium at the Moon is derived from meteorite vaporization of the regolith. Two facts support this result. First, the *Potter and Morgan* [1988*a*] observations show an Na D line FWHM of 42 mÅ corresponding to a temperature of 1000 K as discussed above, and second, *Potter and Morgan* [1988*b*] measured a very extended distribution above the subsolar surface. The measured line shape and vertical scales are basically compatible. We argue that these results leave no room for a significant accommodated component and loss rates must be determined by a large escape fraction. The *Potter and Morgan* [1988*b*] data can be approximated using a single scale height of $H_{Na} = 600$ km, and density at the surface of $[N_{Na}] = 33$ cm^{-3}. This very large scale (an accommodated gas would have $H_{Na} = 80$ km) implies a commensurately very large loss rate. If one considers a thermal Jeans escape loss or alternatively assumes a coronal distribution, the loss rate is roughly

$$S_{Na} - S_{aNa} \approx 30 \times 10^4 \text{ cm}^{-2}\text{s}^{-1} \quad (18)$$

compared to the predicted

$$S_{Na} = 16 \times 10^4 \text{ cm}^{-2}\text{s}^{-1} \quad (19)$$

from Table 3. This interpretation of the data substantially alters the possible value of f_{aNa}. The actual loss rate is not easily determined, because the gas is not Maxwellian. The nature of the observed data makes it a certainty that direct escape loss of Na is a significant quantity, although the exact value of the rate is uncertain.

The *Potter and Morgan* [1988*b*] analysis of these data combined with the earlier data from the discovery paper [*Potter and Morgan*, 1988*a*], assumed that a dominant cold component near the surface temperature was present, with an additional hot component representing source particles. However, both the *Potter and Morgan* [1988*a*] and [1988*b*] observations in spite of large differences in atmospheric scale and several months between measurements, extrapolate to the same brightness at the subsolar point (Figure 1). The

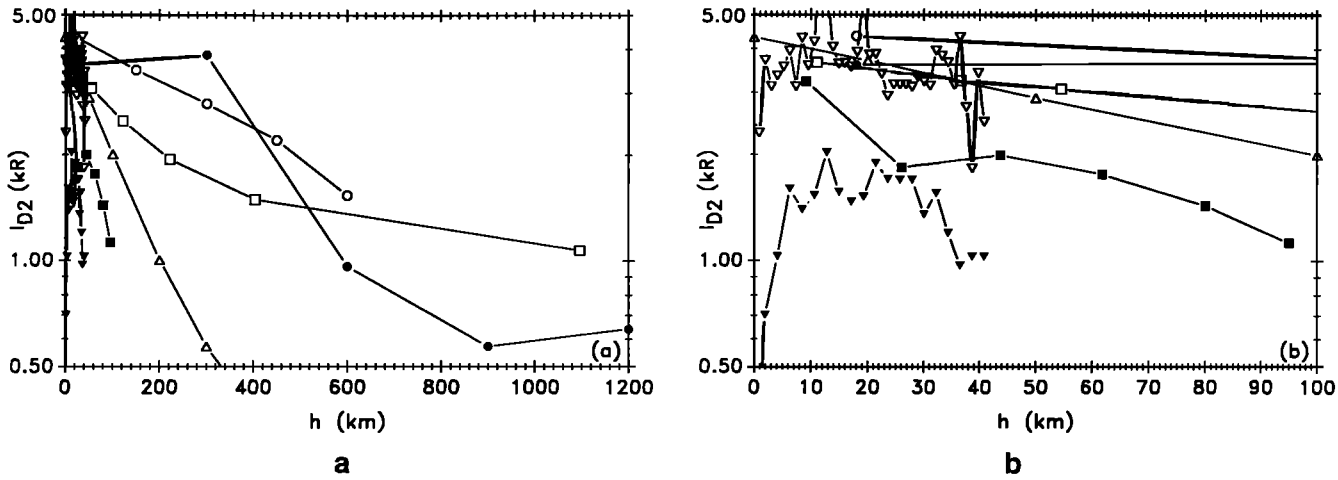

Fig. 1. The sodium and potassium D_2 line brightness (I_{D_2}(kR)) above the bright lunar limb. Open squares show the two scale height barometric model of *Potter and Morgan* [1988*b*], which does not include the effect of Jeans escape. The open triangles show the *Potter and Morgan* [1988*b*] barometric model for a scale height of H_{Na} = 120 km, corresponding to an Na gas temperature T = 540 K. Open circles denote*Potter and Morgan* [1988*b*] Na data on October 2, 1988. Solid circles denote *Potter and Morgan* [1988*b*] Na data on October 3, 1988. Solid squares denote *Tyler et al.* [1988] Na data in June 1988. Open inverted triangles denote *Potter and Morgan* [1988*a*] Na data in January 1988. Solid inverted triangles denote *Potter and Morgan* [1988*b*] K data in February 1987. Figure 1*a* shows the data on a 1200 km scale and Figure 1*b* shows the near limb on a 100 km scale above the lunar surface.

data therefore shows no evidence for a measurable accommodated component. The analysis by *Potter and Morgan* [1988*b*] was biased by the assumption that a substantial equilibrated accommodated component must be present. This argument was influenced mainly by the calculations of Shemansky and Kunc [see *Hunten et al.*, 1988] which show a large accommodation coefficient for Na. However, the physical argument that sodium should accommodate rapidly in physical interaction with the surface is on a solid basis, and we are left with the serious problem of the scale of lunar data as reported by Potter and Morgan. The magnitude of the impasse is illustrated by the fact that if a retention factor f_{aNa} = 0.25 is used as given in Table 3, we predict a subsolar limb brightness in the Na D_2 line of about 15 kR in accommodated gas, compared to the observed value of ~ 4 kR in much hotter gas. The value required to match the observations, $f_{aNa} \sim 0.005$, demands either a very hot source, or a peculiarity in the interaction with the surface. The first possibility appears unlikely given the known parameters of the impact phenomenon. The alternative solution to the dilemma is to argue that a significant fraction of the source sodium at an effective energy equivalent of ~ 4000 K, say, has sufficient energy to overcome the activation barrier to low energy chemical reaction at the surface. The relatively rapid desorption of chemically bound surface Na by solar wind and EUV radiation would again leave the atoms released to the atmosphere in a kinetically hot distribution determined by the activation barrier, establishing in this way a small f_{aNa} in effective competition with a large physical accommodation coefficient. The observations by Potter and Morgan were all directly above the subsolar point, where desorption of atoms in the top surface layer by solar wind and EUV radiation should be maximized. The distribution over the terminators may be quite different, because of the rapid relaxation rate that would occur when the mean energy of the impacting atoms falls below the activation energy at the surface sites.

A complication in the interpretation of the observational data is introduced by the results obtained by *Tyler et al.* [1988], who claim to obtain H_{Na} = 79 ± 8 km [now revised to 75 ± 27 km, A. Sprague private communication, 1990], in contrast to the combined Potter and Morgan data which shows $H_{Na} \sim 600$ km, as discussed above (Figure 1). This presents a clear divergence in measured scale. However there are several factors to consider in weighing the observations. Both the *Potter and Morgan* [1988*a*] and *Tyler et al.* [1988] data were obtained below an altitude of 100 km, and both obtained relatively small scale heights in the analysis, which in the case of Potter and Morgan was shown to be largely in error as discussed above, based on the more extensive *Potter and Morgan* [1988*b*] results. These results define a slope, effectively requiring differentiation of the data, and the estimated uncertainties in our view were unrealistically small in both cases. Although the *Potter and Morgan* [1988*a*, *b*] data are internally consistent, there are serious differences with the *Tyler et al.* [1988] results. The brightness values of *Tyler et al.* [1988] which occur temporally between the Potter and Morgan measurements, are factors of 1.4 and 3.5 lower at the limb and at 100 km, respectively. Strong temporal variability seems unlikely, in view of the consistency of the *Potter and Morgan* [1988*a*, *b*] data. Figure 1 shows a comparison of the data. The *Tyler et al.* [1988] results are in addition subject to larger uncertainty because of the applied calibration method, and the necessity to subtract a large background from the data. The combination of these factors suggests that a single scale height of 600 km is currently the most accurate representation. On this basis the Potter and Morgan data indicate that the loss of Na from the Moon is dominated, not by photoionization but by escape, and that the escape rate could be as much as 2 times the calculated source rate in Table 3. The *Tyler et al.* [1988] results cannot be reconciled with the *Potter and Morgan* [1988*a*, *b*] measurements, particularly at 100 km above the limb. Further measurements are needed to

firmly establish spatial distribution and temporal behavior. The conservatively estimated source rate calculated above requires that the loss rate of the observed sodium be at least 10 times larger than the photoionization rate. This is compatible with the large escape rate implied by the Potter and Morgan data. We therefore argue that the most likely dominant source of Na at the Moon is produced by impact vaporization of the regolith by the steady influx of small meteorite particles. In Table 3 we have assumed a large atmospheric retention factor for this source, which cannot be correct, given the observational data. In other words, we propose that the error in our calculation of atmospheric source rate (S_{aNa}) above lies in the value of the retention factor ($f_{aNa} = 0.25$) rather than the conservatively estimated source rate (S_{Na}). If we accept the *Potter and Morgan* [1988*b*] results as representing the normal atmosphere the value of the retention factor (f_{aNa}) must be reduced by two orders of magnitude ($f_{aNa} \sim 0.005$). The implication of this result is that the vapor temperature of the impact must be near the high end of the laboratory experimental results. The escape energy for Na at the lunar surface is 0.69 eV. In contrast, at Mercury the retention factor for the same process would be significantly larger, since the escape energy for Na there is 2.1 eV. In fact the temperature of the observed sodium at Mercury can be interpreted as accommodated gas. The differences in Na abundances between the Moon and Mercury may in part be attributed to this factor.

The lack of evidence for an accommodated component in the *Potter and Morgan* [1988*a*,*b*] observations raises a consideration of the issue of collisional accommodation of the gas with the surface, as discussed above. It seems very unlikely on a qualitative basis that no accommodated component would be detected unless the reaction of hot Na atoms from the source involved a significant branch for low energy chemistry at the surface. This also appears to be the case in the consideration of the required loss rates for oxygen discussed below.

Oxygen

In the present calculations, the supply of oxygen to the atmosphere is controlled by solar wind and radiation desorption. An additional small amount is obtained from the photolysis of H_2O (see 11). As we point out above the upper limits on source rate based on observation are factors of 1000 and 4000 below our calculated value, assuming that the loss of O is controlled by solar ionization. The disparity of the observational upper limits and the calculated source rate is clearly enormous. If the calculated source is to be considered a reasonable value, it is necessary to assume that the atmospheric loss rate must be significantly higher than inference from photoionization and charge exchange. The required lifetime is of the order of the transport time to the lunar darkside, $\sim$ 1 hour, if we assume a source energy equivalent temperature of $\sim$ 4000 K. A mean energy this large like the case of Na above, would require a significantly large probability for low energy chemical reactions at the surface. Low energy chemistry is known to occur with open Si bonds on damaged SiO_2 amorphous layers[*Carrière and Lang*, 1977], with activation energy of order 0.2 eV. In addition to a relatively large escape rate, similar to Na, we appear to require an additional loss process.

We propose that charge exchange reactions on the darkside may provide the needed loss rate. The cold antisolar lunar surface severely limits chemical reactions. A possible near resonant reaction that we consider here is the charge transfer process described as

$$\text{(R8)} \qquad (surf)^- + O \rightarrow O^- + (surf)$$

The sunlit solar subsurface is charged positive by reaction mainly with solar photons in the subsurface. The reaction path is one of photoionization in which the separated electron is left with sufficient excess kinetic energy to diffuse through the surface to form a space charge in the atmosphere. The positive holes created in the solid are not readily recombined because of the diffusion path and activation barrier presented to the electrons, leaving the sunlit subsurface with a net positive potential. This effect has been established experimentally both in the laboratory [see *Dekker*, 1958] and in in situ measurements on the Moon [see *Manka and Michel*, 1973]. The lunar darkside acquires a net negative charge because of the inability of electrons relaxing to the surface to recombine with the subsurface positive charge. The surface potential on the darkside has been estimated to be ~ -40 eV [*Manka and Michel*, 1973]. The electron affinity of O is $\varepsilon_O = 1.465$ eV. The affinity of Si is $\varepsilon_{Si} = 1.38$ eV, but compounds such as SiH and SiH_2 have lower values of 1.28 eV and 1.12 eV respectively [*Kasdan et al.*, 1975]. It therefore appears quite possible the reaction (R8) could be near resonance or exothermic with excess energy taken up by kinetics in the reaction. The adsorption time for O on an 85 K silicate surface is estimated to be of order 10^{-8} s, allowing significant time for exploration of the surface during the adsorption period. Thus the necessary physical quantities are present for reaction (R8) to have a high probability. On the other hand Na with $\varepsilon_{Na} = 0.4$ eV would encounter a substantial activation barrier for charge transfer if the silicate affinity is $\varepsilon > 1.0$ eV. A rapid loss of O by formation of O^- and subsequent acceleration in the surface field, would therefore not be a viable process for Na. Other species, He for example ($\varepsilon_{He} = -.5$ eV) would also not be limited by this process. However, OH ($\varepsilon_{OH} = 1.8$ eV) could easily experience a similar fast reaction rate to that of O on the darkside, and charge transfer to form OH^- could constitute the limiting rate for loss. Potassium with $\varepsilon_K = 1.$ eV may or may not be affected depending on the exact value of the mean surface molecule electron affinity.

Comparison of the Moon and Mercury

The same physical processes acting to form and destroy the exosphere of the Moon are also expected to occur at Mercury, but at different rates. The known differences are the larger gravitational field and the presence of a planetary magnetic field at Mercury. At the surface of Mercury the escape velocity is 4.4 km s^{-1} as compared to 2.3 km s^{-1} at the surface of the Moon. This difference should lead to a large difference in the retention factor f_{aNa} for Na derived from impact vaporization, and probably, a difference in the retention factor for sputtered species. Based on the discussion above the value of f_{aNa} at the Moon may be as low as $\sim$ 0.005, if the accommodated component is as low as 10% of the total observed sodium abundance. The ratio of f_{aNa} values for Na at Mercury and the Moon may thus be as large as 100. The values of f_a for any species which enters the atmosphere by effusion (^{40}Ar) through the regolith, will not differ significantly.

The effect of the magnetic field is more difficult to assess at this point. In the case of the Na exosphere, we know [*Killen et al.*, 1990; *Potter and Morgan*, 1990]: (1) that there are often local concentrations of sodium at either or both poles [*Potter and Morgan*, 1990]; (2) that the distribution of sodium is not symmetric with respect to luminance coordinates [*Killen et al.*, 1990]; and (3) that the distribution is variable over a time scale of a day [*Potter and Morgan*, 1990]. There is no evidence for similar phenomena in the lunar exosphere. *Killen et al.* [1990] suggest a process modulated by the magnetic field, but simple direction of the some fraction of the interdicted solar wind onto the auroral ovals is not an adequate explanation for the observed phenomenon. Detailed studies of the magnetospheric phenomena which might produce or distribute Na and other species are required.

Finally, one should note that the elemental composition of the regolith of Mercury is not known. Thus a possible explanation for some of the difference between the Moon and Mercury may be simply composition. All three of these differences (escape velocity, phenomena associated with the magnetic field of the planet, and composition) may be important for Na. In the case of O, neither the difference in escape velocities or compositional differences will play a large role. The main effect of the planetary magnetic field would be to modify the local surface charging characteristics at Mercury reducing the effect of charge transfer as a loss process. Thus the large differences in the column densities of O and Na at the Moon compared to Mercury may have separate causes.

Conclusion

Based on our estimation of rate processes and review of observations for the lunar atmospheric constituents of major interest, we have arrived at the following conclusions.

1. The production of sodium and potassium is controlled by impact vaporization of the regolith by meteorites. The calculated rate and observations together indicate that Na and probably K are lost mainly by escape of the hot impact product. The lack of evidence for accommodated gas in the observations suggests that significant rates for low energy chemistry at the surface are required to provide very low values of f_{aNa}. At Mercury where accommodated Na is observed, the larger escape energy implies a much larger retention factor, f_{aNa}. This may account for a significant part of the low abundance of Na on the Moon relative to the value on Mercury.

2. Atomic oxygen is produced mainly by solar wind sputtering and desorption induced by absorption of solar photons. The calculated source rate is at least three orders of magnitude larger than expectation based on observational upper limits and assumed loss by ionization. In order to account for the discrepancy, we propose that low energy chemistry may affect accommodation rates through the desorption of hot O atoms as proposed above for sodium, coupled with an additional loss process of charge transfer on the lunar darkside, to form O^- with subsequent acceleration out of the system. A similar charge transfer process would not be effective for sodium. Potassium may experience a small rate for charge transfer, but OH may be seriously affected by loss through the formation of OH^-.

3. We predict a brightness of the OH 3085 Å band of $\sim$ 50 R at the subsolar limb, assuming the gas is accommodated to the surface temperature and limited by photolysis. This estimate excludes a possible contribution from a small comet source described by *Frank et al.* [1986]. The flux of water onto the Moon due to the *Frank et al.* [1986] small comet source leads to an exosphere and corona containing large amounts of OH and O, with unacceptably large predicted emission rates in OH 3085 Å and O 1304 Å transitions.

4. The possibility of formation of H_2O ice in permanently shadowed regions of the Moon has been reexamined, with the conclusion that the lifetime of the ice layer is limited by LISM H Lyα photodissociation, a process not previously considered. The episodic nature of the comet input may allow the formation of frost deposits in our estimation, providing localized sources of OH.

Appendix A

The velocity distribution of the impact generated gases can be considered in a semiquantitative fashion. The vapor produced as an impact proceeds to its end will show a range of temperatures. The participation of any constituent volatile species will depend on the volatility of that species and whether it is derived from the regolith or from the meteoroid. The prompt vapor production, which is the fraction of the gas for which continuum radiation and line emission are observed in laboratory measurements, is contained in both a spherical vapor cloud which is observed to expand rapidly away from the source, and to a lesser extent, in the high velocity jets of material associated with oblique impacts. The former is likely to be the major vapor loss path. The prompt cloud motion is quite complicated, but a crude approximation to the behavior of the cloud is a dense spherical gas cloud expanding isentropically into a vacuum [*Zel'dovich and Razier*, 1967]. The outermost shell of the cloud expands at a velocity of

$$v_{max} = \frac{2}{\gamma - 1} \cdot \left(\gamma \cdot \frac{P_0}{\rho_0}\right)^{\frac{1}{2}} \tag{A1}$$

where γ is the ratio of the specific heats, P_0 is the initial pressure, and ρ_0 is the initial density. Deeper layers leave with decreasing velocities which approach a limiting velocity, typically a third the velocity of the initial layers. The limiting velocity is approximated by the equation

$$v_{min} = \left(\frac{\gamma - 1}{2\gamma}\right)^{\frac{1}{2}} \cdot v_{max} \tag{A2}$$

We do not know the initial pressure or the initial density; we do have values for the initial temperature associated with the immediate vapor production, approximately 2500 − 5000 K. If we assume that the ideal gas law holds, a mean temperature $T_{ave} \doteq 5000$ K, $\gamma = 1.67$, and mean molecular weight 24 amu, then $v_{max} = 5.1$ km s^{-1} and $v_{min} = 2.3$ km s^{-1}. At $T_{ave} = 5000$ K one would expect that the neutral atomic species dominate. In this approximation most prompt vapor clouds would exceed escape velocity on the Moon. Interestingly, most of this vapor would be retained on Mercury.

The calculation above should be viewed as an upper limit for a small fraction of the vapor produced. Radia-

tive losses are neglected, for example, as are the effects of molecular recombination which will proceed until the expanded cloud becomes collisionless, and the maximum temperature was assumed. A value of $T_{ave} = 2500$ K is compatible with detailed calculations for representative impacts [*Ahrens and O'Keefe*, 1977; *O'Keefe and Ahrens*, 1982]. At lower temperatures the average molecular weight will increase. This suggests that the bulk of the vapor produced by the impact is cooler and has a higher molecular weight. If $T_{ave} = 2500$ K and the mean molecular weight of 60 amu, then $v_{max} = 4.65$ km s^{-1} and $v_{min} = 1.55$ km s^{-1}. A greater fraction of the lower temperature vapor is, of course, retained.

Vapor produced in the early stages of the impact is very hot (perhaps as high as 5000 K) and the vapor derived at later stages as the impact proceeds is typically cooler. The early vapor production can come from the regolith directly under the impact and from the leading edge of the meteoroid which is still moving downward at many km s^{-1}. As the impact continues, larger fractions of the vapor will be derived from increasing volumes of the regolith and the meteoroid that are subjected to an attenuated shock. Vapor in the later stages of the impact is due the devolatilization of melt and shocked solid fractions, and does not participate in the rapid outward expansion described above.

Regolith derived Na and K are most likely to be in the prompt cloud and the most volatile species like H_2O will dominate the late stage vapor production. If the qualitative description presented here is correct, then Na and K are much more likely to be lost from the Moon on impact than are the volatiles like H_2O. An observable result of this physical picture is that the distribution of Na and K above the bright limb of the Moon should extend to great height while the distribution of other volatiles should be much more characteristic of an accommodated gas.

APPENDIX B

The expansion velocities of the vapor cloud formed by the impact of the small comets can be calculated from the expressions in Appendix A (equations (A1) and (A2)). The initial composition of the gas must be specified in order to specify the mean molecular weight, μ, and the average ratio of the specific heats, γ. We examine three initial compositions: (1) H_2O vapor; (2) OH + H; (3) O + H + H. The critical quantities, μ, γ, T, v_{max} (equation (A1)), v_{min} (equation (A2)), and v_{exp} ($[v_{max} + v_{min} - v_{esc}]/2$) are given in Table B1. Since these velocities are greater than the escape velocity, v_{esc}, the three endpoint compositions all predict a corona.

The corona formed by the impact of the small comets is likely to show both spatial and temporal variations near the lunar surface, but these effects become smaller as one moves away from the surface. If we assume a bulk velocity of 4 km s^{-1} for the escaping gas, an altitude of 10 R_M is obtained in $\sim$ 1 h. The estimated impact rate of 52 small comets per hour over the lunar surface implies one impact within a 500 km radius on the surface per hour. The observation of the emission due to any species in the lunar environment requires long exposures, so that inhomogeneities will be averaged out. Thus for the present purpose a spherically symmetric coronal model can be used to calculate the expected distribution of the gas with r, the radial distance from the center of the Moon, and the resulting brightness in a resonance line along any line–of–sight through the gas for any constituent. An additional assumption was made; namely, that the corona can be characterized by a single outflow velocity to the gas (taken to be v_{exp}). This assumption can be easily removed, but to first order there is no major change in the predicted flux, particularly within 4 or 5 radii of the surface of the Moon.

The distribution of OH and O with r is quite different for the different source compositions. The distribution of H_2O for the conditions described above is given by the equation

$$N_{H_2O}(r) = \frac{S_{H_2O}}{v_{exp}} \cdot \left(\frac{r_0}{r}\right)^2 \cdot exp\left[-\frac{r - r_0}{H_{H_2O}}\right] \qquad \text{(B1)}$$

where

$$H_{H_2O} = v_{exp} / \sum_{13}^{17} P_i$$

and r_0 is the radius of the Moon. The values of P_i are given in Table 2, v_{exp} in Table B1, and we obtain a scale height $H_{H_2O} = 154$ R_M. The vertical abundance of H_2O is $\eta_{H_2O} = 5. \times 10^{13}$ cm^{-2}. If the species input to the base of the corona is H_2O, then to a good approximation,

$$N_{OH}(r) = \frac{S_{H_2O}}{v_{exp}} \cdot \left(\frac{r_0}{r}\right)^2 \cdot \left(\frac{P_{13} + P_{14}}{A_z}\right) \cdot \left(exp\left[\frac{r - r_0}{H_z}\right] - 1.\right) \cdot exp\left[-\frac{r - r_0}{H_{OH}}\right] \qquad \text{(B2)}$$

where

$$H_z = \frac{v_{exp}}{A_z} \quad H_{OH} = \frac{v_{exp}}{P_{10} + P_{11}} \quad A_z = (P_{10} + P_{11}) - \sum_{13}^{17} P_i$$

The quantities in Tables 2 and B1 give $H_z = 2200 R_M$ and $H_{OH} = 140 R_M$. If the species input to the base of the corona is OH, then

TABLE B1. Average Lunar Coronal Outflow Velocities for the Small Comet Impact Source

Composition[a]	T,K	μ[b]	γ[b]	v_{max}, km s^{-1}	v_{min}, km s^{-1}	v_{exp} [c], km s^{-1}
H_2O	2500	18	1.286	8.51	2.83	4.5
OH+H	2500	9	1.54	6.96	2.94	3.8
O+H+H	2500	6	1.67	7.81	3.36	4.4

[a] Assumed asymtotic compositions of impact vapor.
[b] See text.
[c] $v_{exp} = \{v_{max} + v_{min} - v_{esc}\}/2.0$.

$$N_{OH}(r) = \frac{S_{OH}}{v_{exp}} \cdot (\frac{r_0}{r})^2 \cdot exp[-\frac{r - r_0}{H_{OH}}] \quad \text{(B3)}$$

For B3, $H_{OH} = 120R_M$.

For case 1 the distribution of O is given by

$$N_O(r) = \frac{S_{H_2O}}{v_{exp}} \cdot (\frac{r_0}{r})^2 \cdot (\frac{(A_u - A_y)}{A_u} \cdot PA \cdot \frac{P_{10}}{A_y} + \frac{P_{15}}{A_y} + \frac{P_{10}}{A_u} \cdot PA \cdot exp[-\frac{r-r_0}{H_u}] - \frac{1}{A_y} \cdot (P_{15} + PA \cdot P_{10}) \cdot exp[-\frac{r-r_0}{H_y}]) \cdot exp[-\frac{r-r_0}{H_O}] \quad \text{(B4)}$$

where

$$H_u = \frac{v_{exp}}{A_u} \quad H_y = \frac{v_{exp}}{A_y} \quad H_O = \frac{v_{exp}}{P_5 + P_6}$$

$$A_u = P_{10} + P_{11} - (P_5 + P_6) \quad A_y = \sum_{13}^{17} P_i - (P_5 + P_6)$$

$$PA = \frac{P_{13} + P_{14}}{A_z}$$

The quantities in Tables 2 and B1 give $H_u = 147R_M$, $H_y = 158R_M$, and $H_O = 6310R_M$.

For case 2 the distribution of O is given by

$$N_O(r) = \frac{S_{OH}}{v_{exp}} \cdot (\frac{r_0}{r})^2 \cdot (\frac{P_{10}}{A_u}) \cdot (1. - exp[-\frac{r-r_0}{H_u}]) \cdot exp[-\frac{r-r_0}{H_O}] \quad \text{(B5)}$$

The quantities in Tables 2 and B1 give $H_u = 124R_M$, and $H_O = 5330R_M$.

The final case, that the species input at the base of the corona is O and H, is more easily treated because the photodissociation rate and the charge exchange rates for O are so small. To first order the density of O near the Moon is just

$$N_O(r) = \frac{S_O}{v_{exp}} \cdot (\frac{r_0}{r})^2 \quad \text{(B6)}$$

and the abundance is given by (3).

In each case, the column and hence the brightness in a line of sight can be calculated by numerical integration. This has been done and the results are shown in Table B2.

TABLE B2. Calculated OH 3085Å and O 1304Å Brightness for the Small Comet Source of Lunar Coronal H_2O Products

r^a R_M	OH(3085Å) kR		OI(1304Å) R		
	H_2O^b	OH+H	H_2O	OH+H	O+H+H
1	0.520	42.9	1.07	17.8	691.
2	0.456	21.1	1.09	18.3	345.
3	0.416	13.8	1.05	17.7	230.
4	0.386	10.2	1.01	17.0	173.
5	0.363	8.0	0.98	16.4	138.
6	0.345	6.6	0.94	15.9	115.
7	0.328	5.6	0.91	15.4	99.
8	0.315	4.8	0.89	14.9	86.
9	0.302	4.2	0.87	14.5	77.
10	0.291	3.7	0.85	14.1	69.
11	0.281	3.3	0.83	13.8	63.
12	0.272	2.5	0.80	13.5	58.

Observations are along a line of sight impact parameter, r. Chemical species refer to assumed initial vapor composition for each column.

[a] Line of sight impact parameter.

[b] Includes dissociative excitation of H_2O, (R13).

Acknowledgments. The authors wish to thank M. Zolensky, A. Potter, P. D. Feldman, M. McGrath, R. Johnson, A. Dessler, R. Killen, D. M. Hunten, and A. Sprague for valuable information and discussion. This work is supported by NASA grant NAG 5-560 to the University of Arizona.

The editor thanks T. M. Donahue and another referee for their assistance in evaluating this paper.

REFERENCES

Ahrens, T. J., and J. D. O'Keefe, Shock melting and vaporization of lunar rocks, *Moon*, *4*, 214–249, 1972.

Ahrens, T. J., and J. D. O'Keefe, Impact and explosion cratering, in *Impact and Explosion Cratering*, edited by D. J. Roddy, R. O. Pepin, and R. B. Merrill, pp. 639–656, Pergamon, New York, 1977.

Arnold, J. R., Ice in the lunar polar regions, *J. Geophys. Res.*, *84*, 5659–5668, 1979.

Barth, C. A., Planetary ultraviolet spectroscopy, *Appl. Opt.*, *8*, 1295–1303, 1969.

Bilrig, J. P., J. P. Chaumont, J. C. Dran, F. Lalu, Y. Langevin, M. Maurette, and B. Vassent, Solar wind and solar flare maturation of the lunar regolith, *Proc. Lunar Sci. Conf., 6th*, 3471–3483, 1975.

Boslough, M. B., R. J. Weldon, and T. J. Ahrens, Impact induced vapor loss from serpentine, nontronite, and kernite, in *Proc. Lunar and Planet. Sci. Conf., 11th*, 2145–2158, 1980.

Carrière, B., and B. Lang, A study of the charging and dissociation of SiO_2 surfaces by AES, *Surf. Sci.*, *64*, 209–223, 1977.

Davis, P. M., Comment on the letter "On the influx of small comets into the Earth's atmosphere", *Geophys. Res. Lett.*, *13*, 1181–1183, 1986.

Dekker, A. J., Secondary electron emission, *Solid State Phys.*, *6*, 251–311, 1958.

Dessler, A. J., The Small–Comet Hypothesis, *Rev. Geophys., in press*, 1991.

Donahue, T. M., T. I. Gombosi, and B. R. Sandel, Cometesimals in the inner solar system, *Nature*, *330*, 548–550, 1987.

Eichhorn, G., Heating and vaporization during hypervelocity particle impact, *Planet. Space Sci.*, *26*, 463–467, 1978.

Fastie, W. G., P. D. Feldman, R. C. Henry, H. W. Moos, C. A. Barth, G. E. Thomas, and T. M. Donahue, A search for far– ultraviolet emissions from the lunar atmosphere, *Science*, *182*, 710–711, 1973.

Fegley, B., and J. S. Lewis, Volatile element chemistry in the solar nebula, *Icarus*, *41*, 439–455, 1980.

Feuerbacher, B., M. Anderegg, B. Fitton, L. D. Laude, R. F. Willis, and R. J. L. Grard, Photoemission from lunar surface fines and the lunar photoelectron sheath, *Geochim. Cosmochim. Acta*, *3*, 2655–2663, 1972.

Florenskiy, K. P., A. T. Basilevskiy, and A. V. Ivanov, The role of exogenic factors in the formation of the lunar surface, in *NASA Conf. Publ. CP–370*, 571–584, 1977.

Frank, L. A., J. B. Sigwarth, and J. D. Craven, On the influx of small comets into Earth's upper atmosphere, II, Interpretation, *Geophys. Res. Lett.*, *13*, 307–310, 1986.

Frank, L. A., J. B. Sigwarth, and J. D. Craven, Reply to Wasson and Kyte, *Geophys. Res. Lett.*, *14*, 781–782, 1987.

Gibson, E. K., S. Chang, K. Lennon, G. W. Moore, and G. W. Pearce, Sulfur abundances and distributions in Mare basalts and their source magmas, *Proc. Lunar Sci. Conf., 6th*, 1287–1301, 1975.

Grinspoon, D. H., and J. S. Lewis, Cometary water on Venus: Implications of stochastic impacts, *Icarus*, *74*, 21–35, 1988.

Hall, D. T., and D. E. Shemansky, No cometesimals in the inner solar system, *Nature*, *335*, 417–419, 1988*a*.

Hall, D. T., and D. E. Shemansky, The evidence against an inner solar system source of atomic hydrogen, *Bull. Am. Astron. Soc.*, *20*, 836, 1988*b*.

Hapke, B., On the sputter alteration of regoliths of outer solar system bodies, *Icarus*, *66*, 270–279, 1986.

Hodges, R. R., and J. H. Hoffman, Molecular gas species in the lunar atmosphere, *Moon*, *14*, 159–168, 1975.

Hodges, R. R., J. H. Hoffman, and D. E. Evans, Lunar orbital mass spectrometer experiment, Apollo 16 Preliminary Science Report, *NASA Spec. Publ., SP–315*, 21–1–21–6, 1972.

Hoffman, J. H., R. R. Hodges, F. S. Johnson, and D. E. Evans, Lunar atmospheric composition experiment, Apollo 17 Preliminary Science Report, *NASA Spec. Publ., SP–330*, 17–1–17–9, 1973.

Hunten, D. M., T. H. Morgan, and D. E. Shemansky, The Mercury atmosphere, in *Mercury*, edited by F. Vilas, C. R. Chapman, and M. S. Matthews, pp. 562–612, University of Arizona Press, Tucson, 1988.

Husinsky, W., et al., Collisional and electronic processes under ion, electron and photon bombardment of alkali and alkaline–earth halides, *Nucl. Instrum. methods Phys. Res., B33*, 824–829, 1988.

Ip, W. H., and J. A. Fernandez, Exchange of condensed matter among the outer and terrestrial protoplanets and the effect on surface impact and atmospheric accretion, *Icarus*, *74*, 47–61, 1988.

Johannessen, J. S., W. E. Spicer, and Y. E. Strausser, An Auger analysis of the SiO_2 –Si interface, *J. Appl. Phys.*, *47*, 3028–3037, 1976.

Johnson, F. S., J. M. Carroll, and D. E. Evans, Lunar atmospheric measurements, *Proc. Lunar Sci. Conf., 3rd*, 2231–2242, 1972.

Johnson, R. E., Application of laboratory data to the sputtering of a planetary regolith, *Icarus*, *78*, 206–210, 1989.

Kasdan, A., E. Herbst, and W. C. Lineberger, Laser photoelectron spectrometry of the negative ions of silicon and its hydrides, *J. Chem. Phys.*, *62*, 541–548, 1975.

Keller, H. U., et al., Comet P/Halley's nucleus and its activity, *Astron. Astrophys.*, *187*, 807–823, 1987.

Killen, R. M., A. E. Potter, and T. H. Morgan, Spatial distribution of sodium vapor in the atmosphere of Mercury, *Icarus*, *85*, 145–167, 1990.

Knotek, M. L., and P. J. Feibelman, Ion Desorption by Core–Hole Auger Decay, *Phys. Rev. Lett.*, *40*, 964–967, 1978.

Knotek, M. L., and P. J. Feibelman, Stability of ionically bonded surfaces in ionizing environments, *Surf. Sci.*, *90*, 78–90, 1979.

Knotek, M. L., V. O. Jones, and V. Rehn, Photon–stimulated desorption of ions, *Phys. Rev. Lett.*, *43*, 300–303, 1979.

Kouchi, A., Vapour pressure of amorphous H_2O ice and its astrophysical implications, *Nature*,*330*, 550–552, 1987.

Kyte, F. T., and J. T. Wasson, Accretion of extraterrestrial matter: Ir deposited 33 to 67 million years ago, *Science*, *232*, 1225–1229, 1986.

Langseth, M. G., S. J. Keihm, and K. Peters, Revised lunar heat flow values, *Proc. Lunar Sci. Conf., 7th*, 3143–3171, 1976.

Lanzerotti, L. J., W. L. Brown, and R. E. Johnson, Ice in the polar regions of the Moon, *J. Geophys. Res.* , *86*, 3949–3950, 1981.

Manka, R. H., and F. C. Michel, Lunar ion energy spectra and surface potential, *Geochim. Cosmochim. Acta*, *3*, 2897–2908, 1973.

McDonnell, J. A. M., Accretionary studies on Apollo 12054,58: In situ lunar surface microparticle flux rate and solar wind sputter rate defined, *Proc. Lunar Sci. Conf., 8th*, 3835–3857, 1977.

McGrath, M. A., R. E. Johnson, and L. J. Lanzerotti, Sputtering of Sodium on the planet Mercury, *Nature*, *323*, 694–696, 1986.

Morgan, T. H., H. A. Zook, and A. E. Potter, Production of sodium vapor from exposed regolith in the inner solar system, *Proc. Lunar Planet. Sci., 19*, 297–304, 1989.

O'Keefe, J. D., and T. J. Ahrens, Impact ejecta on the Moon, in *Proc. Lunar Planet. Sci. Conf., 7th*, 3007–3025., NASA, 1976.

O'Keefe, J. D., and T. J. Ahrens, Meteorite impact ejecta: Dependence of mass and energy loss on planetary escape velocity, *Science*, *198*, 1249–1251, 1977*a*.

O'Keefe, J. D., and T. J. Ahrens, Impact–induced energy partitioning, melting, and vaporization on terrestrial planets, *Proc. Lunar Sci. Conf. 8th*, 3357–3374, 1977*b*.

O'Keefe, J. D., and T. J. Ahrens, Cometary and Meteorite swarm impact on planetary surfaces, *J. Geophys. Res.*, *87*, 6668–6680, 1982.

Potter, A. E., and T. H. Morgan, Discovery of sodium and potassium vapor in the atmosphere of the Moon, *Science*, *241*, 675–680, 1988*a*.

Potter, A. E., and T. H. Morgan, The extended sodium exosphere of the Moon, *Geophys. Res. Lett.*, *15*, 1515–1518, 1988*b*.

Potter, A. E., and T. H. Morgan, Evidence for magnetospheric effects on the sodium atmosphere of Mercury, *Science*, *248*, 835–838, 1990.

Quaide, W., and V. Oberbeck, Developement of the mare regolith: Some model considerations, *Moon*, *15*, 27–55, 1975.

Schramm, L. S., D. E. Brownlee, and M. M. Wheelock, Major element composition of stratospheric meteorites, *Meteoritics*, *24*, 99–112, 1989.

Schultz, P. H., Experimental impact research,*Int. J. Impact Eng.*, *5*, 569–576, 1987.

Sigmund, P., Sputtering by ion bombardment: Theoretical concepts, in *Sputtering by Particle Bombardment* , Vol. I, edited by R. Behrisch, pp. 9–71, Springer–Verlag, New York, 1981.

Sprague, A. L., A diffusion source for sodium and potassium in the atmospheres of Mercury and the Moon, *Icarus*, *84*, 93–105, 1990.

Tolk, N. H., R. G. Albridge, A. V. Barnes, and D. P. Russell, Final–state determination in interactions of directed energetic photon and particle beams with surfaces, *Conf. Ser. Inst. Phys., 94, Sect. 12*, 385–390, 1988.

Tolk, N. H., and T. S. Larchuk, Photon and electron desorption of atoms and molecules from surfaces, *Conf. Ser. Inst. Phys., 71*, 135–142, 1984.

Tuncel, G., and W. H. Zoller, Atmospheric iridium at the south pole as a measure of the meteoritic component, *Nature*, *329*, 703–705, 1987.

Tyburczy, J. A., and T. J. Ahrens, Dehydration kinetics of shocked serpentine, in *Proc. Lunar Planet. Sci. Conf., 18th*, 435–441, Cambridge University Press., 1988.

Tyburczy, J. A., B. Frisch, and T. J. Ahrens, Shock induced volatile loss from a carbonaceous chondrite: Implications for planetary accretion, *Earth Planet. Sci. Lett.*, *80*, 201–207, 1986.

Tyler, A. L., R. W. H. Kozlowski, and D. M. Hunten, Observations of sodium in the tenuous lunar atmosphere, *Geophys. Res. Lett., 15*, 1141–1144, 1988.

Wasson, J. T., and F. T. Kyte, Comment on the letter "On the influx of small comets into the Earth's atmosphere, II,: Interpretation", *Geophys. Res. Lett., 14*, 779–780, 1987.

Watson, K., B. C. Murray, and H. Brown, The behavior of volatiles on the lunar surface, *J. Geophys. Res.*, *66*, 3033–3041, 1961.

Wendell, W. W., and F. J. Low, Low–resolution differential drift scans of the Moon at 22 microns, *J. Geophys. Res.*, *75*, 3319–3324, 1970.

Wu, C. Y. R., and D. L. Judge, Multichannel processes of H_2O in the 18 eV region, *J. Chem. Phys.*, *89*, 6275–6282, 1988.

Zel'dovich, Ia. B., and Yu. P. Raizer, *Physics of shock Waves and High Temperature Gases*, Academic, San Diego, Calif., 1967.

T. H. Morgan, National Aeronautics and Space Administration, 600 Independence ave., SW, Washington, D. C. 20546.

D. E. Shemansky, Lunar and Planetary Laboratory-W, University of Arizona, Gould-Simpson Building, Rm 927, Tucson, AZ 85721.

(Received January 8, 1990;
revised August 20, 1990;
accepted September 17, 1990.)